Wear 440–441 (2019) 203104

Contents lists available at ScienceDirect

Wear

journal homepage: http://www.elsevier.com/locate/wear

Sub-stoichiometric oxides for wear resistance

M. Woydt

BAM Federal Institute for Materials Research and Testing, Unter Den Eichen 87, 12200, Berlin, Germany

ARTICLE INFO

Keywords:
Sub-oxide
Friction
Wear
Carbide
Tribo-oxidation
Cermet
Hardmetal
Titanium
Niobium
Magnéli
Block structures
Planar defects

ABSTRACT

Sub-stoichiometric oxides formed by tribo-oxidation were often analyzed in tribofilms, like γ-Ti_3O_5, Ti_5O_9 and Ti_9O_{17} and $Mo_{0,975}Ti_{0,025}O_2$ as well as double oxides, like β-$NiMoO_4$ or $NiTiO_3$. Thus, the contribution of sub-oxides with planar defects (Ti_nO_{2n-1}, $Ti_{n-2}Cr_2O_{2n-1}$) or as block-structures ($Nb_{3n+1}O_{8n-2}$) to the tribological profile of carbides by using monolithic oxides is of scientific interest and has model character.

The tribological profiles of these model oxides under dry unidirectional sliding have shown, that sub-oxides have a contribution to the tribological behavior of carbides and cermets, when they are tribo-oxidatively formed, because their tribological profiles as monolithic materials are homologuous in part or totally, or compete with hardmetals or cermets, depending from the operating conditions regarded.

1. Introduction

Tribo-oxidation prevents adhesive wear, reduces wear and sometimes also friction, but the tribo-reactive layers are difficult to analyze, because they are thin, of amorphous or nano-crystalline nature. The tribological tests with polycrystalline and monolithic model materials are much more comprehensive and conclusive as hypothesis from surface analysis, because they are “ab initio” present in a pre-defined form and will not be formed by tribo-oxidation as uncontrolled process on non-oxide surfaces. Substances, that were analyzed in wear tracks/scars and/or believed to be formed by tribo-oxidation were realized as pure solid model substances and their tribological profile was compared to substrates (non-oxides) on which they were formed by tribo-oxidation. Additionally, a monolithic material can’t be worn down to the substrate and no substrate interferes with the tribological test data. Consequently, the main direction of this paper is the summarize the experimental data of “monolithic model materials”,

a. If they exhibit more anti-wear and/or more lubricious (low-frictional) properties and
b. If their specific defect structures can act as explanations for the exceptional tribological behavior of these mainly carbidic substrates.

2. Surface oxides

2.1. Lubricious oxides

Coming from liquid lubricants and greases, low friction and wear were attributed to the use of lubricants. In 1988 Gardos [1] used the term ‘lubricious oxides’ to describe expected low coefficients of friction (COF) and wear rates in unlubricated dry sliding conditions for titanium suboxide (TiO_{2-x}) materials, as he expected low lattice energy crystallographic shear systems in oxygen-deficient rutile.

Historically, at the beginning nineteen-eighties, the experimental evidences in tribological tests with different humidities and as function of the oxygen partial pressure as well as by means of surface analysis revealed, that oxide layers exercise a beneficial effect on the tribology of TiN and TiC coatings [2] as well as ceramic-ceramic composites (SiC–TiC, Si_3N_4–TiN) [3,4] and cermets ((Ti,Mo) (C,N)–15NiMo) [5]. Materials containing the element titanium in phases such as titanium nitride or titanium carbide, or solid solutions of these (i.e., titanium carbonitride), are characterized by a high wear resistance. The tribo-oxidative formation of reaction layers composed of [CS]-structures [5] of γ-Ti_3O_5, Ti_5O_9, Ti_9O_{17} and $Mo_{0,975}Ti_{0,025}O_2$ as well as double oxides $NiTiO_3$ and β-$NiMoO_4$ determined their tribological profile.

Reactions occurring as result of tribological sollicitations in air lead to the formation of different surface oxides existing in the Ti–O phase

E-mail addresses: mathias.woydt@bam.de, m.woydt@matrilub.de, mathias.woydt@bam.de.

https://doi.org/10.1016/j.wear.2019.203104
Received 3 December 2018; Received in revised form 25 October 2019; Accepted 25 October 2019
Available online 1 November 2019

diagram [6,7]. Titanium dioxide (TiO_2) is the most important oxide, having several modifications. Rutile is the most stable modification. Another important modification of TiO_2 is anastase, which irreversibly transforms into rutile during heating. The good wear resistance of titanium-containing materials is connected with the tribologically induced formation of the sub-stoichiometric titanium oxides TiO_x with $1.66 < x < 2.0$ [8].

2.2. Sub-stoichiometric oxides

Binary systems of metal and oxides form sub-stoichiometric oxides, which accommodate the oxygen deficiency in different manners:

a. Planar defects (TiO_2, MoO_3, WO_3)
The oxygen deficiency is accommodated by homologous series (Magnéli-type phases) of ordered structures with (132) crystallographic shear planes, which represent planar oxygen defects and can be described through the formula Ti_nO_{2n-1} with even n in the range between 4 and 10, but also up to 19 [9,10]. "n" is the plane spacing (distance) between the (132) CS planes. Molybdenum and tungsten oxides form similar homologous series of Me_nO_{3n-2}. The stability against re-oxidation of Ti_nO_{2n-1} begins in air between 370-400 °C and can be enhanced by chromia. On the titania-rich side of the phase diagram of the TiO_2–Cr_2O_3, homologous series of $Ti_{n-2}Cr_2O_{2n-1}$ as solid solution are formed, which are structurally isomorphous with the Magnéli phases Ti_nO_{2n-1} of the Ti–O system. In TGA analysis, $Ti_{n-2}Cr_2O_{2n-1}$ is stable in air until 1.500 °C [11].
b. Block-structures (Nb_2O_5, V_2O_5)
The ideal or undistorted structure of Nb_2O_5 can be broken up into different groups of octahedron arrangements. The blocks are composed of NbO_6-octahedra arranged in groups of 3×3 and 3×4 or 3×5 or 2×5 sharing octahedron edges with each other [12]. These blocks enable different local arrangements within the crystal. Stoichiometric and monoclinic Nb_2O_5 is the member with $n = 9$ of a possible series of structural homologues [13] expressed by $Nb_{3n+1}O_{8n-2}$. Based upon the block-structure principle, sub-stoichiometric phases as structural homologues to Nb_2O_5 can be assumed to have the same symmetry and unit cell dimensions, when $n = 5$ and $n = 7$, which results in the compounds $Nb_{22}O_{54}$ ($NbO_{2,454}$) and $Nb_{16}O_{38}$ ($NbO_{2,375}$). This complicates the phase analysis by x-ray diffraction techniques. The oxygen loss (deficiency) is accommodated in the boundaries between the blocks.
$Nb_{22}O_{54}$ ($n = 7$, $NbO_{2,45}$) and *o*-$Nb_{12}O_{29}$ ($n = 4$, orthorhombic, $NbO_{2,42}$) are two examples of reduced Nb_2O_5 and share a common motif [14] of symmetry-equivalent 4×3 blocks of corner sharing NbO_6 octahedra, whereas 3×3 blocks are also present in $Nb_{22}O_{54}$. Grühn [15] et al. illuminated that in $Nb_{12}O_{29}$ the 3×4 blocks can be linked to an orthorhombic or monoclinic symmetry.

Common for both types of sub-oxides with planar defects or block structures is the electrical conductivity, as the oxygen deficiency is accommodated in "crystallographic shear" (CS) planes by a change in valence of the metal atom. Niobium cations change the oxidation level from pentavalent (Nb^{5+}) to tetravalent (Nb^{4+}) and titanium cations from Ti^{4+} to Ti^{3+}.

It has to be noted, that other metallurgical systems, like vanadized metallic surfaces, hardmetals based on tungsten carbide, sprayed molybdenum coatings and TiN as well TiC have outstanding wear resistances and are all able to form sub-oxides or Magnéli-type oxides through tribo-oxidation. Both, titania and pentavalent niobium oxide have high melting points without any tendency to sublimate, like WO_3 or MoO_3. Nb_2O_5 has a melting point of 1522 °C and titania melts at 1855 °C.

2.3. Monolithic sub-oxides

The term 'lubricious oxides' [1,6] was introduced to tribology in order to describe expected low coefficients of friction (COF) and high wear resistances in unlubricated (dry) sliding conditions. Numerous studies were carried out on bulk materials in the Ti–O system [16], like binary Ti_nO_{2n-1} [8], with $4 \leq n \leq 19$, and ternary $Ti_{n-2}Cr_2O_{2n-1}$ (with $6 \leq n \leq 9$) systems [17], as well as Nb–O system ($Nb_{3n+1}O_{8n-2}$, when n is odd) [18], which represent sub-oxides formed as a result of tribo-oxidative and/or high-temperature reactions.

Polycrystalline samples of hot-pressed (HP) $60Ti_4O_7 40Ti_5O_9$ and Ti_6O_{11} and hot-pressed $Ti_2Cr_2O_7$ as well as spark plasma sintered (SPS) $Nb_{12}O_{29}$ ($NbO_{2,4167}$) were synthesized as monolithic model materials.

These model oxides displayed in Table 1 were either hot-pressed or spark plasma sintered to full density. As the strength values lie in the range of magnesium and some aluminium alloys in combination with their micro-hardnesses above those of quench and tempered steels make clear, that these oxides have sufficient strength to resist shear loads. The hardnesses indicate rather a potential for wear resistance than for reduction of friction. In consequence based on the materials properties, it can be predicted, that they contribute rather to wear protection than to lower dry friction. The bulk shear strength is not low enough to respect low friction.

3. Tribological properties

3.1. Tribological test equipment

The tribometers for unidirectional sliding are custom designed developments of BAM and the design details of which are disclosed elsewhere [20]. They do, however, comply with ASTM G99 (or DIN 50324) and with DIN EN 1071–13:2010. The aim is to establish the tribological profile of tribocouples for "closed" tribosystems". After the tests, the wear scar diameters a and b of the toroid were measured under a microscope with a micrometer stage. The particular sample shape used leads to elliptical wear scars with a b/a-ratio of 1.87 in the ideal case. The observed fluctuations in the b/a-ratio were between 1.80 and 1.94 for all of the materials examined. The measured scar diameters on the toroid a and b can be transformed to a linear height (wear) $h_{a,b}$ of the calotte by using the following Eq. (1)

$$h_{a,b} = \frac{D_{a,b}}{2} - \sqrt{\left(\frac{D_{a,b}}{2}\right)^2 - \left(\frac{d_{a,b}}{2}\right)^2} \quad (1)$$

where D_a is the toroid sample radius parallel to the wear scar diameter a, in mm, and D_b is the toroid sample radius parallel to the wear scar diameter b, in mm. d_a and d_b are the measured wear scar diameters on the toroid in mm. As control, the linear wear heights of the calotte h_a and h_b must be equal. From these values, the wear volume W_v [20] on the toroid can be calculated with Eq. (2):

Table 1
Properties of sub-stoichiometric, monolithic model oxides [8,18,19].

Sub-oxide	Elastic Modulus at RT [GPa]	Poisson ratio	Micro-hardness HV0.2	4-point bending strength S_0 [MPa]
Method	ASTM E1875		DIN ISO 6507-1	DIN EN 843-1
$60Ti_4O_7 40Ti_5O_9$ (HP)	221	0,275	930 ± 66	107 ± 21
Ti_4O_7 (HP)	223	0,295	1194 ± 30	212 ± 22
$Ti_7Cr_2O_{17}$/ $Ti_6Cr_2O_{16}$ (HP)	216	–	1350 ± 91	237 ± 38
$Ti_2Cr_2O_{17}$ (HP)	203	0,280	1014 ± 92	290 ± 34
$Nb_{12}O_{29}$ (SPS)	155	0,310	643 ± 30	120 ± 12

$$W_v = \frac{\pi}{6} h^2 \left(3\sqrt{2D_a + 2D_b - h}\sqrt{2D_b - h} + h\right) \quad (2)$$

for 0≪h≪D_b, with $D_a = 15$ mm and $D_b = 6$ mm.

The wear volumes of the rotating disks were determined by stylus profilometry perpendicular to the sliding directions at fours positions every 90° as planimetric wear area W_q in µm^2. The average W_q from four readings is multiplied with the wear track length in order to obtain the wear volume of the disk in mm^3.

The wear coefficients (rate), k_v, is defined as the ratio of volumetric wear [mm^3] to the product of load, F_n [N], and the sliding distance, s [m]. The coefficient of friction (CoF) and the total linear wear of both tribo-elements (specimen) as well as the relative humidity and the sample temperature were recorded continuously. One repeat per combination of parameters was performed, because the testing philosophy at BAM is to screen over a wide range of operating conditions rather than doing repeated tests, except at specific points.

Sintered alumina (99.7%) bodies were used as stationary spherical (toroids with $R_1 = 6/21$ mm and $R_2 = 21$ mm) specimens with polished surfaces ($R_{pk} = 0.019$ µm), which were pressed against the planar surfaces of the rotating disks by a dead weight of $F_N = 10$ N. Alumina is used as stationary specimen, because hot spot temperatures can't initiate in alumina phase transitions and tribo-oxidation. The initial, average (mean) Hertzian contact pressure (P_{0mean}) ranged for a normal force of 10 N from approximately 420 MPa for Al_2O_3/Nb_2O_5 to 725 MPa for Al_2O_3/WC grades. The sliding distance was 1000 to 5000 m, depending from the year of execution. Older results were run under s = 1000 m through s = 2000 m and later ones under s = 5000 m. Experiments were performed at 22 °C and 400 °C in air (rel. humidity at RT for dry sliding approx. 25–40%) with sliding velocities of 0.1, 0.3, 1.0, 3.0 and 7.5/8.0 m/s. The resolution limit of the wear coefficient (rate) for the rotating specimen is approximately 10^{-8} mm^3/N·m.

3.2. Friction and wear coefficients

The following tribological data under dry friction were compared with homologous results achieved in BAM's high temperature tribometers [20] issued from the tribological data base TRIBOCOLLECT of BAM for thermally sprayed coatings [11,21], self-mated ceramics and ceramic composites [4] as well as mated with stationary specimen in alumina [20]. The figures contains in total more than 1160 tribological data sets and use the total wear coefficients, which is the sum of the wear coefficient of the stationary tribo-element #1 (toroid) and the rotating disk (tribo-element #2). For the wear coefficients (rates) of the tribo-elements (toroid or disk) can be found in the cited references. The relative humidities ranged in the dry sliding tests between 25 and 40%.

3.2.1. Oxides

The friction and wear coefficients of materials plotted in Fig. 1 and Fig. 2 were taken from BAM's tribological database TRIBOCOLLECT. The processing, properties and tribological results of the following oxides were published previously elsewhere:

a. Y_2O_3–ZrO_2 and MgO–ZrO_2 [22]
b. TiO_2 [16]
c. Al_2O_3 [20]
d. Cr_2O_3 [17]
e. $TiO_{1,73}$ ($60Ti_4O_7 40Ti_5O_9$) [8].
f. Nb_2O_5 ($Nb_{12}O_{29}$) [18].

Fig. 1 displays remarkable low and stable frictional properties for the couples TiO_2/TiO_2 at room temperature and for Al_2O_3/Cr_2O_3 at 400 °C, but both are outperformed at high velocities and 400 °C by Al_2O_3/Nb_2O_5 ($Nb_{12}O_{29}$).

Relative humidity is at RT a factor on tribological properties. Klaffke [8] found for alumina dry oscillating against TiO_2, $60Ti_4O_7 40Ti_5O_9$ and Ti_6O_{11}, that the wear coefficients dropped under dry oscillation from 20-30 10^{-6} mm^3/N·m at 2% of relative humidity (r.h.) down to 0,5–2, 0 10^{-6} mm^3/N·m at 98% r.h., whereas the coefficients of friction were more or less unaffected and greater than >0,55. Similar behavior was seen for self-mated zirconia [23,24] and for the tribocouple

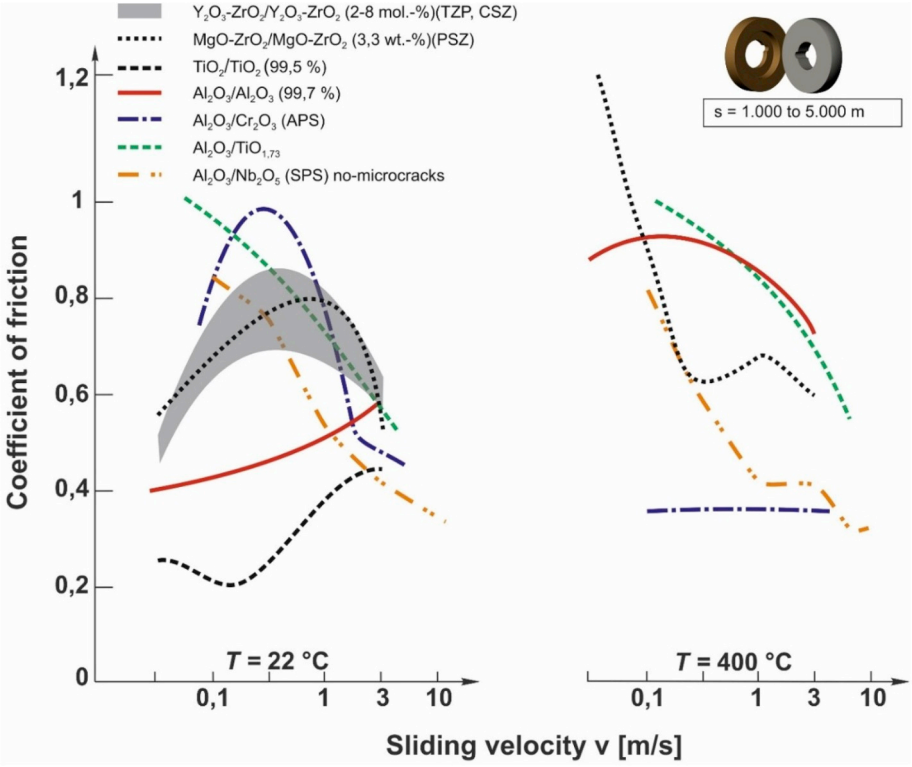

Fig. 1. Evolutions of coefficients of friction of oxides and suboxides under dry friction at RT and 400 °C.

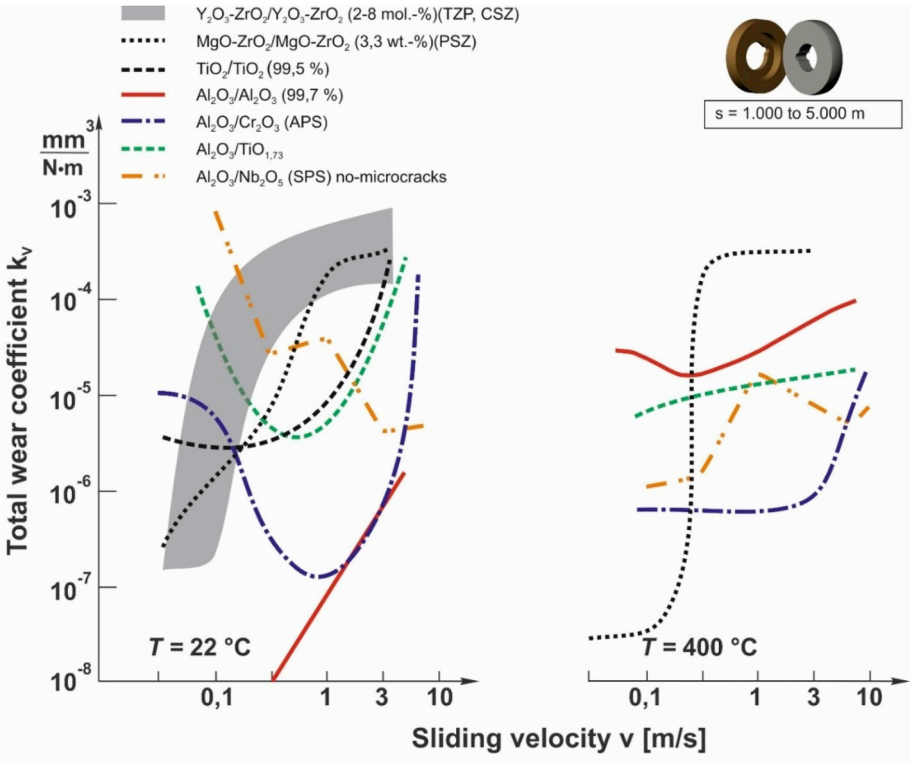

Fig. 2. Evolutions of the total wear coefficients of oxides and sub-oxides under dry friction at RT and 400 °C.

Al_2O_3/Nb_2O_5 ($Nb_{12}O_{29}$) [18].

In contrast for self-mated alumina, friction and wear coefficients under dry oscillation are more or less invariant to relative humidity [23, 24].

Low coefficients of friction, which increased with increasing sliding velocity, can be related to hydrated surfaces. Water and/or H_2O add atoms desorb due to hot spot temperatures with increasing sliding velocity with the consequence, that friction goes up.

As function of sliding speed and temperature, the wear coefficients of oxides in Fig. 2 cover more than five orders of magnitude and the ranking between these depends from the operating conditions. The increase in wear for self-mated zirconia and alumina is related to the hot-spot temperature. In the case of MgO–ZrO_2, the hot spot temperatures reach and exceed the stability region of the cubic phases [22]. The phase transformation of monoclinic and/or tetragonal zirconia to cubic zirconia generates residual tensile stresses and cracks [22]. Alumina has a much higher thermal diffusivity than zirconia and undergoes no phase transitions, but the strong crystallographic anisotropy of elastic modulus times thermal expansion coefficient generates residual stresses between the grain boundaries. The binary phase diagrams of Ti–O (TiO_2), Nb–O (Nb_2O_5) and Cr–O (Cr_2O_3) indicate also no tribologically relevant phase transitions with increasing ambient temperatures, which will generate thermal induced residual stresses.

Nb_2O_5 ($Nb_{12}O_{29}$) is in the sliding velocity range regarded the only oxide so far, where the wear coefficients decreased with increasing sliding speed, even coming from high values at low sliding velocities.

3.2.2. *Oxides versus carbides*

Nitrides, borides and carbides, especially the later, dominate in the arena of wear protection. Different models (Rabinowicz, Evans&Marshall, Zum Gahr, Habig/Woydt) use hardness as the key property determining abrasive wear resistance in “opened” tribosystems, aside toughness and elastic modulus. In “closed” tribosystems, were the surfaces of triboelements meet each other periodically, nitrides, borides and carbides are also dominating, but abrasive particles are mainly not involved. In consequence, the role of hardness on wear resistance can be questioned and also, if tribo-oxidation plays a role on tribological quantities. Tribo-oxidation will imply oxides and what is the intrinsic tribological profile of such sub-oxides?

Fig. 3 displays a simultaneous decline in coefficients of friction with increasing sliding velocity at 22 °C and 400 °C in air for niobium oxide ($Nb_{12}O_{29}$) and several metal bonded NbC-based cermets. On the other hand, the coefficients of friction of niobium oxide ($Nb_{12}O_{29}$) and binderless HP-NbC1 (hot-pressed) evoluvated at RT differently with increasing sliding velocity. The properties of HP-NbC1 can be found in Ref. [25]. In consequence, the friction reducing effect of a niobium oxide film on binderless NbC at RT can’t be only attributed to tribofilms in niobium oxide. In contrast, binderless NbC, Nb_2O_5 and metal bonded NbC grades displayed all a uniform evolution in friction at 400 °C and in wear coefficients at RT and 400 °C, which is consequently dominated by tribo-oxidation.

The wear rates at 22 °C of niobium oxide ($Nb_{12}O_{29}$) (See Fig. 3) plunged downward under dry sliding by two orders of magnitude (200×) when increasing sliding velocity from 0.1 m/s to 7 m/s. At 7 m/s, the wear rate of $4.9\,10^{-6}$ mm^3/N·m for $Nb_{12}O_{29}$ is close to those of the NbC-based cermets, when comparing with Fig. 4 and Fig. 5. The wear rates of binderless NbC and metal bonded NbCs at 22 °C and 400 °C were similar, but those of binderless NbC were at the lower end of metal bonded NbCs. Overall, the much higher strengths and hardnesses of NbC cermets not serve as explanations for the similar wear rates between NbC cermets and $Nb_{12}O_{29}$ at 400 °C or high velocities at RT. In terms of wear rates and in view of binderless NbC with modest four point bending strength of S_0 of 370 MPa, the wear rates are rather dominated by NbC as carbide as by tribo-chemically formed oxides from 8-12 vol -% of metallic binders, like cobalt, nickel or Fe_3Al. The wear coefficients of $Nb_{12}O_{29}$ (See Fig. 3) were at 400 °C low until 0.3 m/and lower than to those of NbC cermets.

At RT, the evolution in coefficients of friction of $60Ti_4O_7 40Ti_5O_9$ in Fig. 4 is different from titanium-based cermets ((Ti,Mo) (C,N)) and WC-based harmetals, whereas at 400 °C the friction drops with increasing

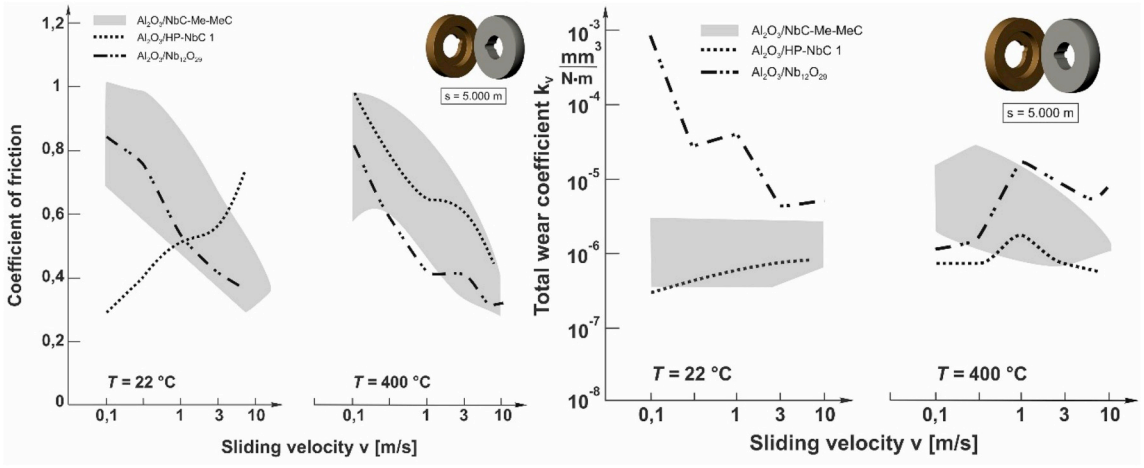

Fig. 3. Coefficients of friction and wear coefficients under dry sliding for $Nb_{12}O_{29}$ and NbC-based cermets [18,25–27].

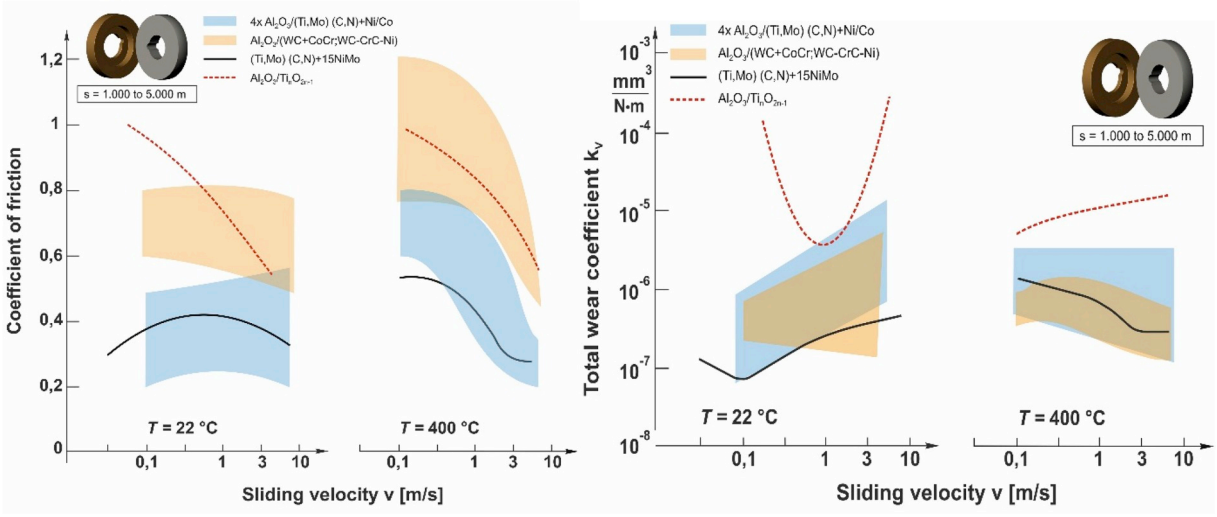

Fig. 4. Coefficients of friction and wear coefficients under dry sliding for Ti_nO_{2n-1}, (Ti,Mo) (C,N) cermets and WC-based hardmetals.

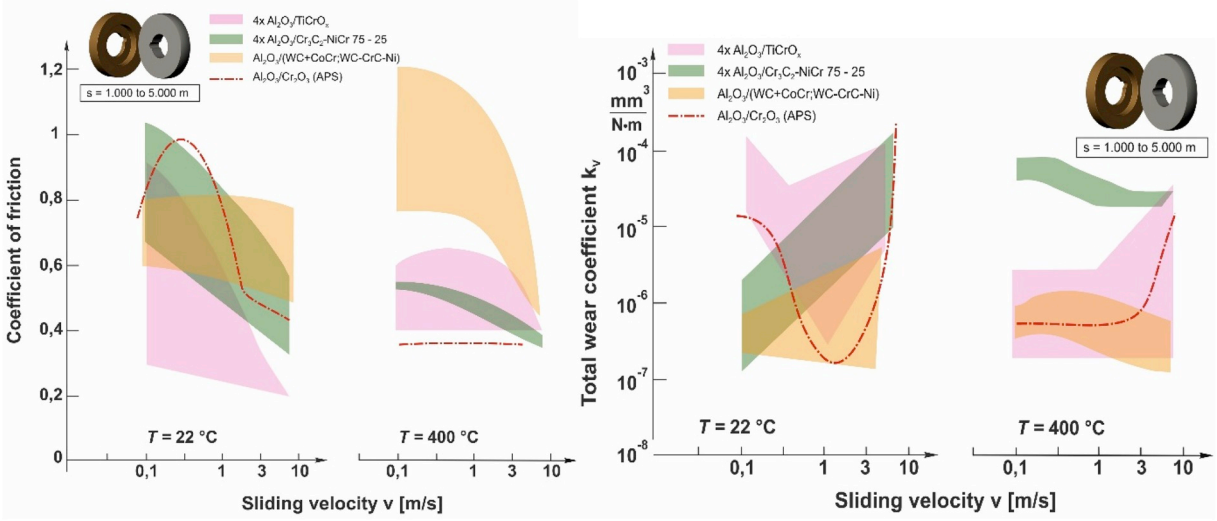

Fig. 5. Coefficients of friction and wear coefficients under dry sliding for $Ti_{n-2}Cr_2O_{2n-1}$, Cr_2O_3 and hardmetals.

sliding velocity for titanium-based cermets ((Ti,Mo) (C,N)), WC-based harmetals and $60Ti_4O_7 40Ti_5O_9$. In comparison to NbC, the tribo-oxidative reaction rate for Ti&W-based substrates is at RT much lower limiting the formation of oxide films. Especially titanium-based cermets form a thin passive reaction layer limiting oxidation up to 1.000 °C, where NbC specimen begins above 500–600 °C to fully convert over time into Nb_2O_5.

The strength and hardness of titanium-based cermets and WC-based hardmetals determine the wear resistance at 22 °C and despite their much lower strength and hardness (see Fig. 4), the Magnéli-type $TiO_{1,73}$ presented at 400 °C a wear resistance independent from sliding velocity and close to those of titanium-based cermets and WC-based hardmetals.

The coefficients of friction for chromium-based systems, either as oxides or carbides, decreased in Fig. 5 with increasing sliding velocity except and surprinsingly, for chromia at 400 °C, where the coefficients of fricton were invariant from sliding velocity. 400 °C seemed to be a convenient operating temperature for chromia, because also the wear coefficients until 3 m/s were invariant against sliding velocity. The impact of tribo-oxidation on wear resistance of chromium-based systems is different:

a. In air and in a general conclusion, the wear coefficients ranged between 10^{-5} and 10^{-4} $mm^3/N{\cdot}m$:
   - for Cr_3C_2 at 400 °C including hot-spot temperatures ΔT with increasing sliding velocity above 22 °C and
   - at 22 °C for $Ti_{n-2}Cr_2O_{2n-1}$, where as
b. 400 °C stabilized the wear resistance for chromia and sub-stochiometric $Ti_{n-2}Cr_2O_{2n-1}$ to around 10^{-6} $mm^3/N{\cdot}m$ and below.

It is visual from Fig. 5, that tribo-oxidation is not beneficial for Cr_3C_2, even Cr_2O_3 displayed much lower wear coefficients. Tribo-oxidation as mechanism for chromia and $Ti_{n-2}Cr_2O_{2n-1}$ (or $TiCrO_x$) is unlikely, because at 400 °C, chromia can't further oxidize and sub-stochiometric $TiCrO_x$ is stable against re-oxidation until >1000 °C [11]. At 400 °C, chromia and sub-stochiometric $TiCrO_x$ competed in terms of wear coefficients with WC hardmetals.

4. Discussion

The monolithic sub-oxides displayed similar evolutions of friction and/or wear coefficients as function of sliding velocity at a given ambient temperature (22 °C or 400 °C) as the cermets and hardmetals prone to tribo-oxidation. The discussion remains complex, because a wide range of sliding velocity between 0.03 m/s to 10 m/s at 22 °C and 400 °C is compared. In a closed tribosystem, not only hardness and elastic modulus (in terms Hertzian contact pressure and stresses), but also thermal diffusivity impacts on the strength, toughness and phase composition of the tribomaterials as well as the thermal diffusivity and expansion on thermal induced, short term/transient residual stresses.

The resulting friction force F_f is defined by equation (3):

$$F_f = \tau_s \cdot A \cong \frac{\tau_s \cdot F_n}{H(T)} \quad (3)$$

where A is the real contact area, F_N is the normal force, τ_s is the shear strength of the thin oxide layer and H(T) is the hardness of the substrate at a given temperature. The yield stress could substitute the hardness.

The hot hardnesses of the sub-oxides can't be compared between each other, as they are still unknown, as well as the evolution of their elastic modulus with temperature. Likely is, that the hardness, which is linked to the shear strength, will drop with temperature and less for carbides than for oxides. Independent from the shear strength of the thin oxide layer, the elastic moduli of carbides (E_{RT} for NbC ~400–440 GPa, E_{RT} for WC ~670–720 GPa) are much higher as those of sub-oxides (See Table 1). In consequence, the real contact area A of carbides is ~$(E_{oxide}/E_{carbide})^{2/3}$ (for point contact) smaller as for the monolithic sub-oxides. Assuming the same metallurgy and properties for the sub-oxides and for tribo-oxidatively on carbides formed sub-oxides results in lower friction forces for the later case. This has to be taken into consideration when comparing the coefficients of friction in air between monolithic sub-oxides and carbides. The elastic moduli at RT of aluminas range between 340-380 GPa and those for chromia (Cr_2O_3, eskolaite) around 280 GPa. Thus at an assumed iso-shear strength and operating conditions, the contact mechanics through the elastic modulus determines the relative level of friction force, either between the oxides and for carbides as well as oxide films formed on carbides.

Alumina (Al_2O_3, corundum) is one of the hardest tribomaterial widely used, but Al_4C_3 (~1200 HV) plays as its carbide no role in tribology, may be due to its sensitivity to hydrolysis. Both, chromia (Cr_2O_3, >2400 HV) and chromium carbide (Cr_3C_2, 1600–2000 HV) are well known for coatings. The micro-hardness of the sintered TiO_2 was determined as 677 ± 70 HV0.2 and 643 ± 30 HV0.2 for Nb_2O_5 ($Nb_{12}O_{29}$). In between ranged the Magnéli-type phases with 930–1130 HV0.2 for Ti_nO_{2n-1} and 1000–1350 HV0.2 for ternary $Ti_{n-2}Cr_2O_{2n-1}$ (see Table 1). It is obvious by comparing these figures of hardness and those of strength and modulus with the evolutions and rankings in wear coefficients shown in Figs. 3–5, that the micro-hardness not serves as a key quantity to comprehend alone the different evolutions in wear coefficients.

In general, the oxides tested here have at 22 °C (RT) a lower thermal conductivity as their related carbides and especially as carbides. $MgO–ZrO_2$ (PSZ, $\lambda_{RT} = 2.1$ W/m·K) [22] and $3{\cdot}Y_2O_3–ZrO_2$ (3Y-TZP, $\lambda_{RT} = 2.2$ W/m·K) [22] have the lowest thermal conductivity followed by TiO_2 ($\lambda_{RT} = 3.2$ W/m·K) [16] with expected similar hot spot temperatures as for $MgO–ZrO_2$. In the case of self-mated $MgO–ZrO_2$, the hot spot temperatures calculated ($F_N = 10$ N, ten micro-asperities) at 1 m/s to max. ΔT = 1800 K and at 3 m/s to max. ΔT = 2200 K [22]. On one side elastic modulus, hardness and strength will degrade under such high hot spot temperatures, but can't be quantified due to a lack of such material's data as function of temperature. This situation is more pronounced for the monolithic sub-oxides. In individual cases, the hot spot temperatures.

a. Trigger phase transitions (e.g. zirconia) and/or
b. Generates residual tensile stresses and cracks, either as
   - residual stresses between the grain boundaries in the case of significant crystallographic anisotropies in elastic modulus and thermal expansion coefficient (e.g. alumina) or
   - transient residual stress gradients between surface and sub-surface area.

Taken all together indicate, why for the oxides the friction (see Fig. 1) decreased at 22 °C with increasing sliding speed and after a specific onset velocity also the wear coefficients (see Fig. 2). It is just in this approach surprising, that the evolution of wear coefficients for Nb_2O_5 ($Nb_{12}O_{29}$), the oxide with the lowest thermal conductivity of ~1 W/m·K and elastic modulus (155 GPa), decreased with increasing sliding velocity. One may allocate this to any accommodation mechanisms related to "block" structures, but is not confirmed by $60Ti_4O_7 40Ti_5O_9$ with "planar" defects.

Cr_2O_3 (λ_{RT}~ 14 W/m·K) [28] and Al_2O_3 (99,5%, $\lambda_{RT} = 28$ W/m·K) [16] have similar thermal conductivities λ as the non-oxides (carbides) NbC-xxMe ($\lambda_{RT} = 16–20$ W/m·K) and Cr_3C_2 ($\lambda_{RT} = 20–23$ W/m·K), what reduces the transient thermal stresses in the micro-asperities. For alumina, a crystallographic thermal mismatch is responsible for the transition to the high wear region [20].

The cermets (Ti,Mo) (C,N)+xxMe ($\lambda_{RT} = 50–60$ W/m·K) and WC ($\lambda_{RT} =$ W/m·K) have the highest thermal conductivities.

5. Conclusions

The friction and wear behavior under dry unidirectional sliding of

different oxides, sub-stoichiometric binary and ternary oxides as well as metal bonded carbides were compared. The presented metallurgical range offered a broad spectrum in hardness (600–2000 HV0.2), in elastic modulus (155–700 GPa), thermal conductivity (1–100 W/(m·K), but the quantities enabled no relations to the tribological profile (friction and wear coefficients) and likely due to the circumstance of testing in a wide range of sliding velocities and at two temperatures as well as tribo-oxidation predominates.

Model oxides have shown under dry unidirectional sliding clear evidences, that sub-oxides have a contribution to the tribological behavior of carbides and cermets, but it remains to the reader, if the evidences are conclusive enough that block structures and planar defects in sub-stoichiometric binary and ternary oxides, as an obvious distinction to oxides and carbides, exert on tribological quantities or in part. Finally, one can certainly appraise total wear coefficients of sub-oxides under dry sliding in air below 10^{-6} mm^3/N·m or 10^{-7} mm^3/N·m at 22 °C and 400 °C, especially at high sliding velocities.

Acknowledgements

The assistance over the years of Ms. Sigrid Binkowski for carefully performing metallography, as well as recording optical and SEM micrographs is gratefully acknowledged.

References

[1] M.N. Gardos, The effect of anion vacancies on the tribological properties of rutile (TiO_{2-x}), Tribol. Trans. 31 (4) (1988) 427–436.
[2] K.-H. Habig, Chemical vapor deposition and physical vapor deposition coatings: properties, tribological behaviour and applications, J. Vac. Sci. Technol. A 4 (6) (1986) 2832–2843. Nov./Dec.
[3] K.-H. Habig, M. Woydt und, A. Skopp, Dry friction and wear of self-mated sliding couples of SiC-TiC and Si_3N_4-TiN, Wear 148 (1991) 377–394.
[4] A. Skopp, M. Woydt, Ceramic and ceramic composite materials with improved friction and wear properties, Tribol. Trans. 38 (2) (1995) 233–242.
[5] M. Woydt, A. Skopp, I. Dörfel, K. Wittke, Wear engineering oxides/Anti-wear oxides, Int. J. Wear 218/1 (1998) 84–95.
[6] M.N. Gardos, H.-S. Hong, W.O. Winer, The effect of anion vacancies on the tribological properties of rutile (TiO_{2-x}), Part II: experimental evidence, Tribol. Trans. 22 (No.2) (1990) 209–220.
[7] H. Mohrbacher, B. Blanpain, J.-P. Celis, J.R. Roos, Raman spectroscopy on defective wear debris generated by contact vibrations, J. Mater. Sci. Lett. 14 (1995) 279–281.
[8] M. Woydt, Tribological characteristics of polycrystalline titaniumdioxides with planar defects, Tribol. Lett. 8 (No. 2–3) (2000) 117–130. Special issue „Lubricious Oxides“.
[9] A. Magnéli, Structures of the ReO_3-type with recurrent dislocations of atoms: „Homologous series“ of molybdenum and tungsten oxides, Acta Crystallogr. 6 (1953) 495–500.
[10] S. Anderson und, A. Magnéli, Diskrete Titanoxydphasen im Zusammensetzungsbereich $TiO_{1,75}$-$TiO_{1,90}$, Die Naturwissenschaften, Jahrgang 43 (Heft 21) (1956) 195–196.
[11] L.-M. Berger, C.C. Stahr, S. Saaro, S. Thiele, M. Woydt, Development of ceramic coatings in the Cr_2O_3-TiO_2 system (bilingual), Therm. Spray Bull. 2 (No.1) (2009) 64–77.
[12] K. Naito, T. Matsui, Review on phase equilibria and defect structures in the niobium-oxygen system, Solid State Ion. 12 (1984) 125–134.
[13] B.M. Gatehouse, A.D. Wadsley, The crystal structure of the high temperature form of niobium pentoxide, Acta Crystallogr. 17 (1964) 1545–1554.
[14] T. McQueen, Q. Xu, E.N. Andersen, H.W. Zandbergen, R.J. Cava, Structures of the reduced niobium oxides $Nb_{12}O_{29}$ and $Nb_{22}O_{54}$, J. Solid State Chem. 180 (2007) 2864–2870.
[15] B. Meyer und, R. Grühn, Oxydationsprodukte von monoklinen $Nb_{12}O_{29}$, elektronenoptische Untersuchungen, Z. Anorg. Allg. Chem. 484 (1982) 53–76.
[16] M. Woydt, *Ti-O — ein Stoffsystem mit erscheinungsreichen tribologischen Eigenschaften (Ti-O* — a materials system with appearance-rich tribological properties), DGM-Tagung „Reibung und Verschleiß“, 09.-11.03.2004, Fürth, ISSN: 0933-5137 (print), 1521-4052 (online), in: Materialwissenschaft und Werkstofftechnik, vol. 35, 2004, pp. 817–823. No. 10.
[17] L.-M. Berger, C.C. Stahr, S. Saaro, S. Thiele, M. Woydt, N. Kelling, Dry sliding up to 7.5 m/s and 800°C of thermally sprayed coatings of the TiO_2–Cr_2O_3 system and (Ti, Mo)(C,N)-Ni(Co), Wear 267 (2009) 954–964.
[18] S.G. Huang, J. Vleugels, H. Mohrbacher, M. Woydt, Densification and tribological profile of niobium oxide, Wear 352–353 (2016) 65–71.
[19] D. Spaltmann, M. Hartelt, M. Woydt, Triboactive materials for dry reciprocating sliding motion at ultrahigh-frequency, Wear 266 (1–2) (2009) 167–174.
[20] M. Woydt, K.-H. Habig, High temperature tribology of ceramics, Tribol. Int. 22 (1989) 75–88.
[21] L.-M. Berger, S. Saaro, M. Woydt, *(*WC-(W,*Cr)$_2$C-Ni*) — the unknown hardmetal coating, Therm. Spray Bull. (2008) 39–42.
[22] M. Woydt, J. Kadoori, H. Hausner und, K.-H. Habig, Unlubricated tribological behaviour of various zirconia based ceramics, J. Eur. Ceram. Soc.. 7 (4) (1991) 123–130.
[23] A. Krell, D. Klaffke, Effect of grain size and humidity on fretting wear in fine-grained alumina, Al_2O_3/TiC and zirconia, J. Am. Ceram. Soc. 79 (5) (1996) 1139–1146.
[24] D. Klaffke, Fretting wear of ceramics, Tribol. Int. 22 (No. 2) (April 1989) 89–101.
[25] M. Woydt, H. Mohrbacher, Friction and wear of binder-less niobium carbide, Wear 306 (1–2) (2013) 126–130.
[26] M. Woydt, H. Mohrbacher, The tribological and mechanical properties of niobium carbides (NbC) bonded with cobalt or Fe_3Al, Wear 321 (2014) 1–7.
[27] S. Huang, J. Vleugels, H. Mohrbacher, M. Woydt, Microstructure and tribological performance of NbC-Ni cermets modified by VC and Mo_2C, Int. J. Refract. Metals Hard Mater. 66 (August 2017) 188–197.
[28] R.K. Williams, R.S. Graves, D.L. McLeroy, Thermal conductivity of Cr_2O_3 in the vicinity of the neel transition, J. Am. Ceram. Soc. 67 (7) (July 1984) C151–C152.